Chapter 2

Sensors for rain measurements

Patrick Willems[1] and Thomas Einfalt[2]

[1]KU Leuven, Hydraulics and Geotechnics, Urban and River Hydrology and Hydraulics, Leuven, Belgium
[2]Hydro & meteo GmbH, Lübeck, Germany

ABSTRACT

Rain measurements based on rain gauges, disdrometers, weather radars and microwave links provide essential input data for urban drainage and stormwater modelling, management, and planning. Their quality strongly depends on the sensor type and calibration, but also on the data post-processing that includes quality control and data adjustment after comparison with reference observations. This chapter provides an overview of traditional techniques and recent developments, and practical advice on the selection of the type of instrument, the installation and calibration aspects to be considered, and the measurement data processing and adjustment needs.

Keywords: Disdrometer, metrology, rainfall, rain gauge, weather radar.

SYMBOLS

a	numerical coefficient in the Marshall-Palmer formula
b	numerical coefficient in the Marshall-Palmer formula
f_{HH}	phase of the horizontally polarized radar reflectivity
f_{VV}	phase of the vertically polarized radar reflectivity
K_{dp}	specific differential phase
L_{dr}	linear depolarization ratio
R	rainfall intensity (m/s)

doi: 10.2166/9781789060119.002_0011

Z radar reflectivity (m^3)
Z_{dr} differential reflectivity
Z_{HH} horizontally polarized radar reflectivity
Z_{VV} vertically polarized radar reflectivity
ρ_{hv} co-polar correlation coefficient

Key messages on sensors for rain measurements

- KM 2.1: *Local vs. global* – rain gauges and disdrometers measure the rain locally while radars can measure over the full catchment.
- KM 2.2: *Calibration* – all devices require calibration. Radar data must be adjusted with local measurements.
- KM 2.3: *Location* – pay attention to the location where the device will be set up to avoid or reduce bias in measurements.

2.1 INTRODUCTION

Rainfall is a key driving force in urban drainage and stormwater management (UDSM) as it generates runoff, in- and ex-filtration, discharges and floods. Its measurement is thus of paramount importance, at timescales ranging from a few minutes (runoff processes and discharges at catchment scale and in UDSM facilities) to decades (statistics on rainfall regime and local climate), for a diversity of actions (system operation, planning, design, modelling, etc.).

Precipitation is mainly measured with rain gauges or/and weather radars, but other measurement techniques exist as well. Where these are unavailable, satellite data may be helpful. This chapter mainly focuses on rain gauges and radars. However, disdrometers and microwave links will be briefly introduced.

2.2 RAIN GAUGES

Rain gauges provide rainfall registrations at ground level or nearby, depending on the height of the rain gauge installation, e.g. in a ground pit, at the ground surface, on a roof top, etc. Rain gauges typically provide measurements of liquid precipitation mass (e.g. in grams) collected on the receiving area of the gauge, during a certain duration. Given the surface of the collecting area, the duration and the amount of water, that information on mass can be converted into rainfall depth (in mm or L/m^2) or rainfall intensity (in mm/h or $L/h/m^2$). In order to measure solid precipitations (such as snow or ice fall), the rain gauges can be heated to melt those precipitations and, therefore, measure them as equivalent liquid precipitation. There are several types of rain gauges:

- Weighing rain gauges (Figure 2.1(a), (c) and (d), WR).
- Tipping bucket rain gauges (Figure 2.1(b), TBR).
- Rainfall height recording gauges (Figure 2.2, only old installations).
- Graduated cylinders.
- Simple buried pit collectors (Figure 2.3).

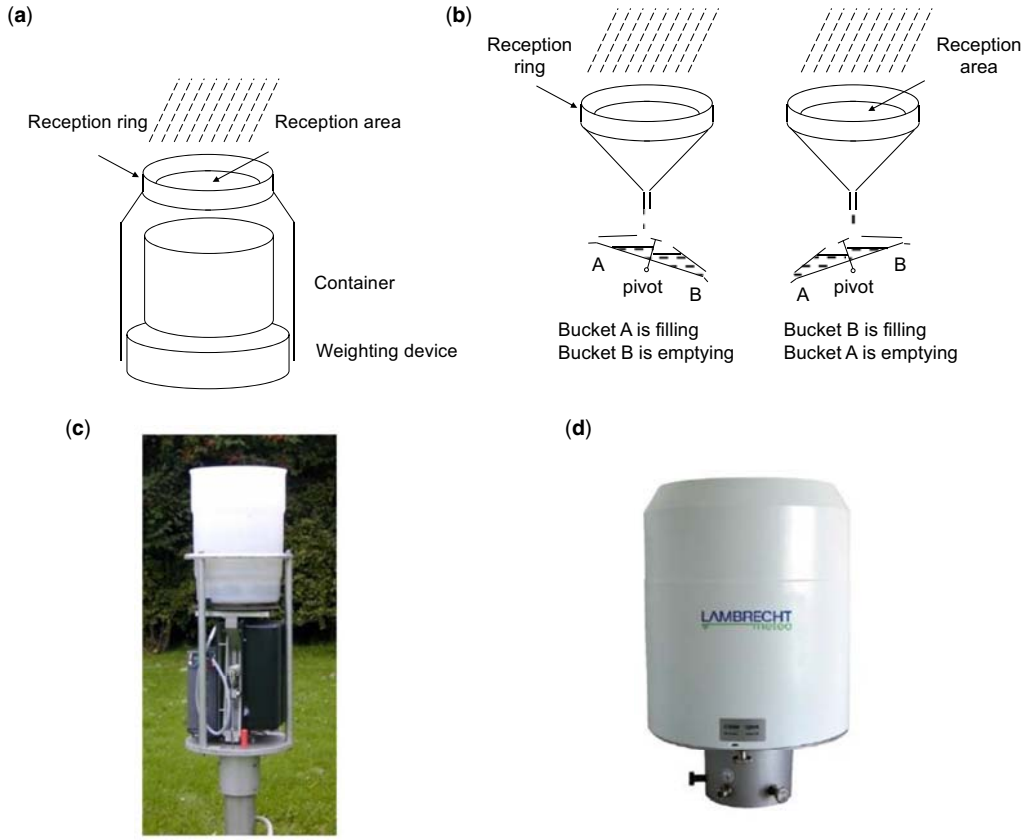

Figure 2.1 Rain gauges: Principles (a) WR, (b) TBR), open (c) and closed (d) WR. *Source:* (a) and (b) adapted from Bertrand-Krajewski *et al*. (2000); (c) Thomas Einfalt, (hydro & meteo GmbH); (d) http://www.lambrecht.net.

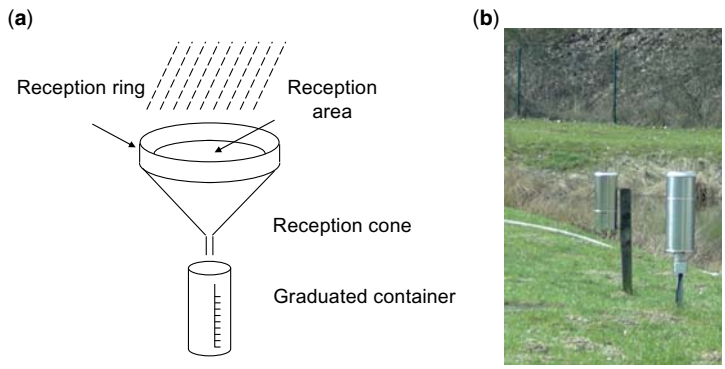

Figure 2.2 (a) Manual rain gauge principle and (b) a closed one as installed in the field. *Source*: (a) adapted from Bertrand-Krajewski *et al*. (2000); (b) Thomas Einfalt (hydro & meteo GmbH).

Figure 2.3 Pit rain gauges or collectors. *Source*: Thomas Einfalt (hydro & meteo GmbH).

WR and TBR (Figure 2.1) offer automatic measurements, which lead (depending on the device and its settings) to a measurement up to every minute. WR have a storage bin for the liquid precipitation, which is weighed to record the mass of water by using a vibrating wire connected to a data logger. Thus, the measurement starts at amounts less than 0.01 mm. TBR consist of a reception area that collects the precipitation and brings it through a funnel into a small bucket. When the mass of the rainwater collected in the bucket exceeds a given value, the bucket tips, actuating a switch (such as a reed switch) which is then electronically recorded (e.g. in a data logger). Each tip typically corresponds to a rainwater mass which is then converted to an equivalent depth of 0.1 to 0.5 mm, which is also the rainfall depth resolution of the gauge. By counting the number of tips in a given time interval, e.g. 5 or 10 minutes, the rainfall intensity can be calculated. Other, including more advanced, types of rain gauges exist as well, but these are not commonly used yet. This chapter does not aim at giving a complete description of all types of rain gauges; it rather focuses on the practical and relevant aspects for the further use of the meteorological data. More details about different types of rain gauges, their properties and accuracies can be found in (among others): World Meteorological Organization (WMO) (2018a), Sevruk (1996), Strangeways (2007) or Wauben (2006).

The WR have the advantage over the TBR that they do not underestimate high rainfall intensities and require much less maintenance because no regular funnel cleaning is required (no clogging possible) and in winter, snow effects (time delayed recording only after melting) are also not encountered. In addition, WR calibration (see Section 7.6) is also much simpler. These gauges are, however, more expensive than the TBR. TBR are not as accurate as the weighing or other types of rain gauges because: (i) the rainfall may start with a non-empty bucket, and (ii) the rainfall may stop before the bucket has tipped once more. The start and the end of rain events may be inaccurately measured with TBR.

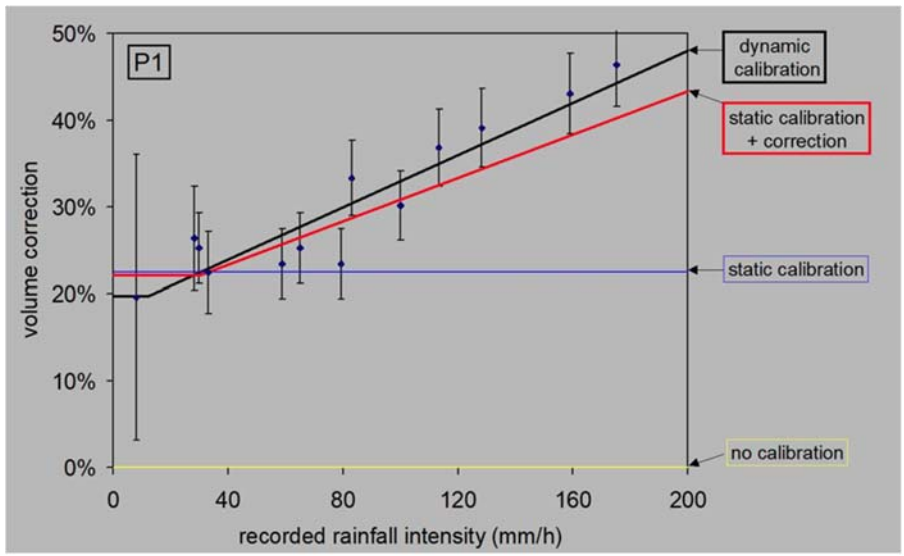

Figure 2.4 TBR gauge calibration, comparing no calibration, static calibration, and dynamic calibration. *Source*: Patrick Willems (KU Leuven).

Moreover, tipping bucket rain gauges typically underestimate the rainfall depths for the higher intensity storms: water can overflow outside the bucket and therefore not be measured. The higher the rainfall intensity, the higher the amount of water lost. Such rain gauges require dynamic calibration to correct for those possible underestimations, depending on the rainfall intensity (Adami & Da Deppo, 1985; La Barbera *et al.*, 2002; Luyckx & Berlamont, 2001; Marsalek, 1981; Niemczynowicz, 1986). Such calibration is often already carried out by the manufacturer. However, a periodic dynamic re-calibration of the rain gauges by the user is necessary (e.g. in Humphrey *et al.*, 1997; Kvicera & Grabner, 2006; Luyckx & Berlamont, 2001), which is preferable compared to the simple static (or volumetric) calibration performed by most manufacturers and users (illustration of the difference in Figure 2.4). Static calibration means that the calibration is carried out with, and hence correction factor(s) are based on, a single test for a given rainfall intensity. Dynamic calibration means that the correction factors are derived by tests at different rainfall intensities, hence as a function of the rainfall intensity (see an example of TBR calibration in Section 7.6.4.6). Several studies (e.g. Habib *et al.*, 2008; Willems, 2001) have shown that these effects can strongly influence the results of runoff simulations.

Rain gauges also have other limitations. First, they only indicate rainfall in a localized area, i.e. the receiving area of the rain gauge which is frequently between 200 and 400 cm^2. Because drops will stick to the sides of the gauge or funnel of the collecting device, rainwater amounts are slightly underestimated for TBR. Moreover, rain gauges are known to encounter difficulties measuring rain in windy conditions (Figure 2.5) as they are mostly not equipped with suitable and necessary windscreens (this causes underestimation, of up to 20%) and can have serious underestimations for high intensity rainfall events (Braak, 1945; Neff, 1977; Sevruk, 1996; WMO, 2018a). The presence of a wind shield or fence on the gauge can reduce this influence (Alter, 1937; Duchon & Essenberg, 2001; Larkin, 1947; Yang *et al.*, 1999); see an example of such a fence in Figure 2.5. Another solution is to level the rain gauge orifice with the ground so that wind effects are minimized, as shown in Figure 2.3.

Figure 2.5 Rain gauge with fence against wind effects. *Source*: Patrick Willems (KU Leuven).

Rain gauges should be placed in an open area where there are no obstacles, such as buildings or trees, to disturb the air flow and corresponding rain conditions. One must also prevent water that has been collected on the roofs of buildings or the leaves of trees from dripping into the rain gauge after a rain event, resulting in inaccurate readings. For rain gauges that measure at ground level, the vulnerability to turbulence is reduced. In this case, the surrounding surface may cause splashing of the raindrops into the gauges and again special care must be given to the selection of the surrounding surface (see Figure 2.3).

Rain gauges with a funnel (especially TBR, but also older recording WR gauges) are sensitive to blockage by e.g. leaves from trees, bird droppings or bird nests. Operational malfunctions could also include failure of the logger or the transmission hard- and/or software. Regular maintenance, check-ups and data validation are highly recommended to check the status of the rain gauge(s). Quality control of the measurement and logging mechanisms of the gauges is strongly advised as well as thorough verification of the rainfall data they provide. Willems (2001) provided an uncertainty assessment for typical TBR measurements in Belgium. Wagner (2009) provided a literature review on the different possible error sources while correcting the rain measurements affecting the TBR measurements and the possible correction methods.

Environmental conditions for rain gauges

Wind, snow and densely constructed area
A densely built-up urban area can affect the rain measurement by increasing or decreasing the amount of rain at the location of the rain gauge. Wind, as a global variable or local effect (in the surroundings of large buildings) can significantly affect rain measurements. If the rain gauge location is prone to freezing conditions or snow events, choose a rain gauge with a melting option.

Local measurements
Rain gauges measure the rain intensity and dynamics at the measuring location. This location should be carefully selected and checked to ensure the recorded data are representative of the catchment of interest.

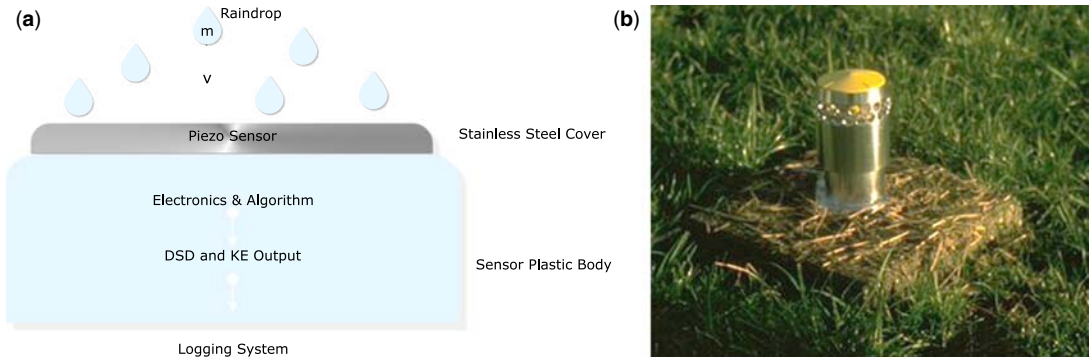

Figure 2.6 Acoustic disdrometers: (a) measuring principle (DSD: drop-size distribution, KE: kinetic energy) and (b) Joss-Waldvogel acoustic disdrometer installed in the field. *Sources*: (a) adapted from Abd Elbasit *et al.* (2011); (b) Thomas Einfalt (hydro & meteo GmbH).

2.3 DISDROMETERS

An alternative way to measure rainfall at the local scale consists of measuring the rain drops with disdrometers. Historically, the first widely used disdrometers were acoustic impact disdrometers (Figure 2.6), measuring the noise generated by the impact of a falling drop and relating this to the rainfall intensity (Joss & Waldvogel, 1967), similar to listening to the rain while driving a car or sitting under a roof window. Nowadays, most disdrometers are optical (Figure 2.7). They are made of one (or several) transmitter(s) and receiver(s) with a sampling volume(s) in between them. The transmitter generates one or several laser sheet(s) and the receiver measures either the occluded light (Battaglia *et al.*, 2010; Frasson *et al.*, 2011; Löffler-Mang & Joss, 2000) or the scattered light (Ellis *et al.*, 2006) from a drop falling through a sampling area of roughly a few tens of cm^2. The received signal is then processed to estimate the size (equivolumetric diameter) and velocity of the hydrometeor which can be a raindrop, a snowflake or a hailstone.

Two-dimensional (2D) video disdrometers have also been developed (Kruger & Krajewski, 2002) but they are not yet used operationally. Some experimental set-ups have also been deployed to reconstruct the 3D raindrop field of frames of a reference volume (1 m^3) (HYDROP Experiment, Desaulnier-Soucy *et al.*, 2001; WMO, 2018a).

Like rain gauges, disdrometers can be biased by wind. The other main limitations are: (i) the estimation of size and velocity of a drop relies on theoretical drop shapes that are often different in reality (Battaglia *et al.*,

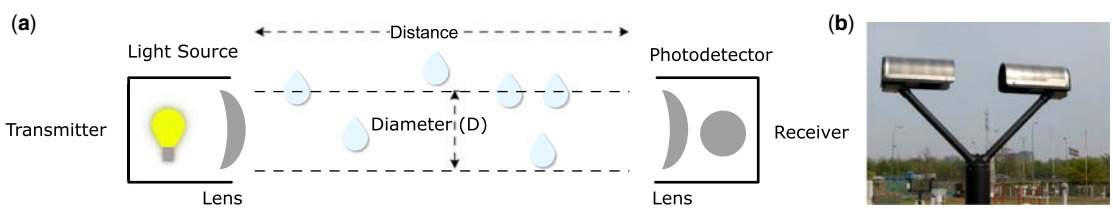

Figure 2.7 Optical disdrometers: (a) measuring principle and (b) example of set-up in the field. *Sources*: (a) adapted from Belenguer *et al.* (2020); (b) Thomas Einfalt (hydro & meteo GmbH).

2010), (ii) a significant sampling error for small time steps occurs because of the small sampling area, up to 15% error in the rain intensity for 1 min time steps and decreasing for larger ones (Jaffrain & Berne, 2012a, 2012b), and (iii) there is a non-homogenous laser beam pattern for disdrometers computing the occluded light (Frasson *et al.*, 2011). Several studies have compared various disdrometers but also compared those disdrometers with more conventional devices such as rain gauges (Brawn & Upton, 2008; Jaffrain & Berne, 2011; Krajewski *et al.*, 2006; Miriovsky *et al.*, 2004; Thurai *et al.*, 2011; Tokay *et al.*, 2001). They concluded that disdrometers are as reliable as the standard devices for point rainfall measurements.

Dense networks of disdrometers have recently been deployed which can show the importance of taking the small-scale drop size distribution variability in the Z-R or R-K_{dp} relation (see Section 2.4.3) into account and more generally of improving knowledge in this field (Jaffrain & Berne, 2012a, 2012b; Tapiador *et al.*, 2010).

2.4 WEATHER RADAR

2.4.1 Introduction

In order to avoid the main disadvantage of rain gauges and disdrometers (local measurement), weather radars (RAdio Detection And Ranging) are nowadays commonly used. Derived from military technology (from World War 2), rain detection replaced aircraft detection: military operators noticed that the images contained echoes from rainfall and other obstacles. After the war, radar technology was further developed, also in a scientific environment, with specific interest for the meteorological use of radar technology.

Radar technology is hereafter discussed in two sections:

- Temporal and spatial resolution of radar data (Section 2.4.2).
- Radar data quality, rainfall estimation, and radar data adjustment (Section 2.4.3).

More information about the measurement principle is presented and detailed in ISO (2019) and WMO (2018b). The contents of the following subsections largely follow the information compiled by Thorndahl *et al.* (2017), with additions from ISO (2019).

2.4.2 Temporal and spatial resolution of radar data

A weather radar (example installations in Figure 2.8) emits microwaves as pulses, and the encountered objects in the atmosphere reflect the emitted microwaves. The radar antenna then measures the amount of reflection and the distance to the radar, based on the travel time of the pulse between emission and reception. Simultaneously, the radar rotates around its axis in order to cover the complete area around a radar site up to the maximum range. To scan the atmosphere in three dimensions, the radar measures at several elevations, i.e. angles pointing into the atmosphere (Figure 2.9).

The microwaves of S, C and X bands are used in most cases and the scale and observation characteristics of the system differ depending on the characteristics of each band (see Table 2.1). S-band systems are large, and their observation range is wide, while X-band systems are compact and their observation range is narrow. The useful, qualitative range of S-band and C-band radars are typically limited by Earth's curvature, whereas at X-band the limit is normally attenuation dependent.

The temporal resolution of radar data is governed by the scanning strategy of the radar. A radar scans the atmosphere at different elevations (Figure 2.9) to generate a full azimuthal volume scan (Figure 2.10). This requires up to several minutes depending on rotational velocity and the number of scanning elevations. A radar collects instantaneous samples of rain intensity estimated from the measured reflectivity, unlike rain

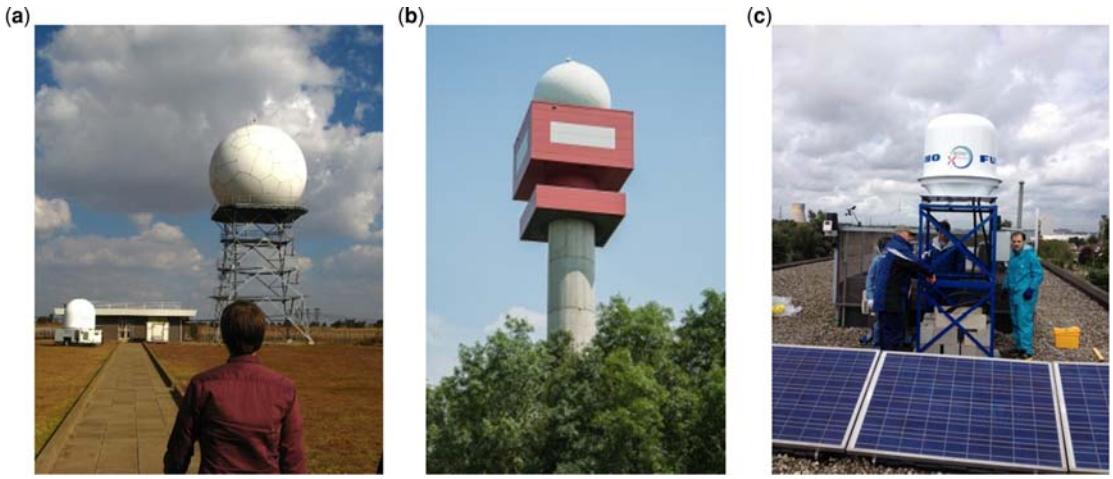

Figure 2.8 Examples of radars. (a) Irene S-band radar of South African Weather Service; (b) C-band radar of Royal Meteorological Institute of Belgium at Jabbeke in Belgium; (c) X-band radar by KU Leuven and Furuno in the city of Gent in Belgium. *Sources*: Thomas Einfalt (hydro & meteo GmbH) and Patrick Willems (KU Leuven).

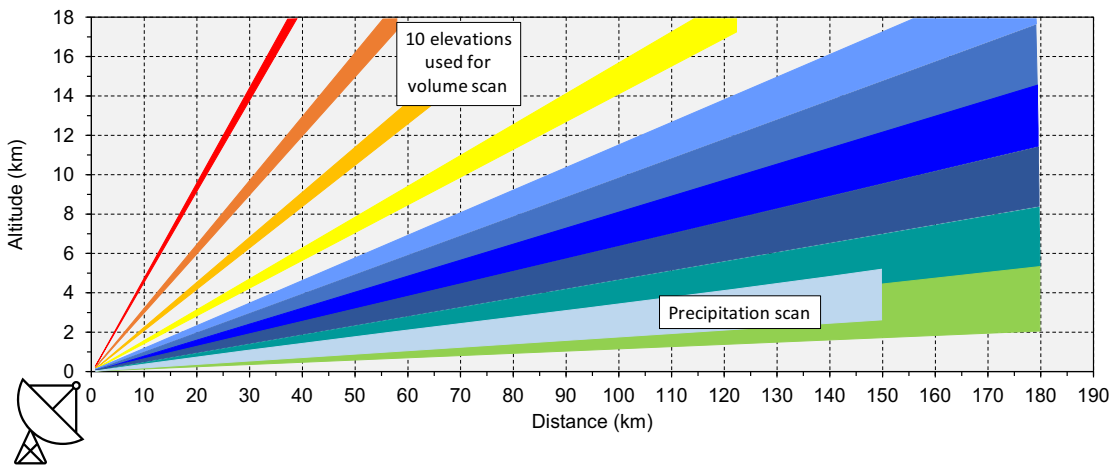

Figure 2.9 Atmospheric scanning strategy of German Weather Service. *Source*: adapted from DWD (2018).

Table 2.1 Typical operating resolutions and maximum ranges for different types of weather radars used in hydrological applications (from Thorndahl *et al.*, 2017).

	X-band	C-band	S-band
Spatial resolution	100–1000 m	250–2000 m	1000–4000 m
Temporal resolution	1–5 min	5–10 min	10–15 min
Maximum quantitative range (see Section 2.4.3)	30–60 km	100–130 km	100–200 km

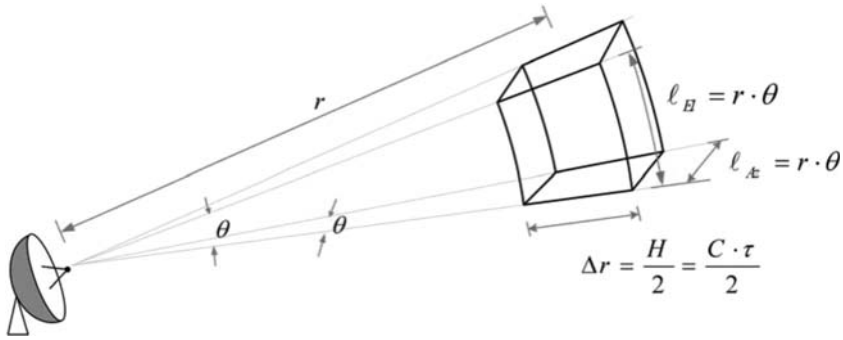

Figure 2.10 Radar scans with radial resolution Δr and azimuthal resolution l_{Az}. *Source*: adapted from Ochoa-Rodriguez *et al.* (2019).

gauges which accumulate rainfall over a given time interval. Some radars operate with intermediate dedicated Doppler scans for each volume scan, hence doubling the time between two consecutive reflectivity scans. Operational meteorological S-, C-, and X-band radars usually provide reflectivity scans with a temporal resolution of 5–15 minutes (Table 2.1), whereas research radars dedicated to high resolution rainfall monitoring in specific areas and specific elevations are reported to provide data resolutions down to 15 seconds (e.g. Mishra *et al.*, 2016; van de Beek *et al.*, 2010).

The main strength of radars for rainfall estimation is their capability to provide spatially distributed rainfall information. The spatial resolution of radar rainfall data is basically determined by the hardware and physics. The radial resolution (or range resolution, Figure 2.10) is a function of the pulse length and for operational radars goes down to 250 m. Radial resolutions between 3 and 100 m have been documented for research radars by e.g. Leijnse *et al.* (2010), van de Beek *et al.* (2010), Lengfeld *et al.* (2014), Mishra *et al.* (2016), Thorndahl *et al.* (2017) and Ochoa-Rodriguez *et al.* (2019).

The spatial resolution also depends on the azimuthal (or angular) horizontal resolution, which is a function of the beam width determined by the size and design of the antenna. In contrast to the radial resolution, the azimuthal resolution (in km) decreases as a function of the radial distance from the radar (Figure 2.10). Most operational weather radars use parabolic dish antennas with a beam width of approx. 1 degree, thus functioning with an azimuthal horizontal resolution close to 1 degree (see http://www.eumetnet.eu/opera, visited the 09/04/2021). As an example, at a distance of 100 km (resp. 55 km) from the radar, the 1° beam is ~1750 m (resp. 1000 m) wide. Small local X-band radars with (non-parabolic) horizontal fan beam antennas typically have larger opening angles between 2 and 3 degrees, but also a smaller maximum range compared to meteorological radars, due to integration of rainfall over a large vertical distance (e.g. Pedersen *et al.*, 2010; Thorndahl & Rasmussen, 2012).

Examples of radar reflectivity maps with four different spatial resolutions covering an approximately 12 km × 12 km area over the city of Aalborg, Denmark, are shown in Figure 2.11. This example illustrates the importance of high spatial resolution data to capture the spatial variability of rainfall which is of critical importance over an urban area (high spatial resolution is important to understand the variability within the urban catchment of rainfall intensities and depth, floods and peak discharges, to better calibrate and test simulation models in particular sewer overflows, etc.) (e.g. Ochoa-Rodriguez *et al.*, 2015, 2019; Rico-Ramirez *et al.*, 2015).

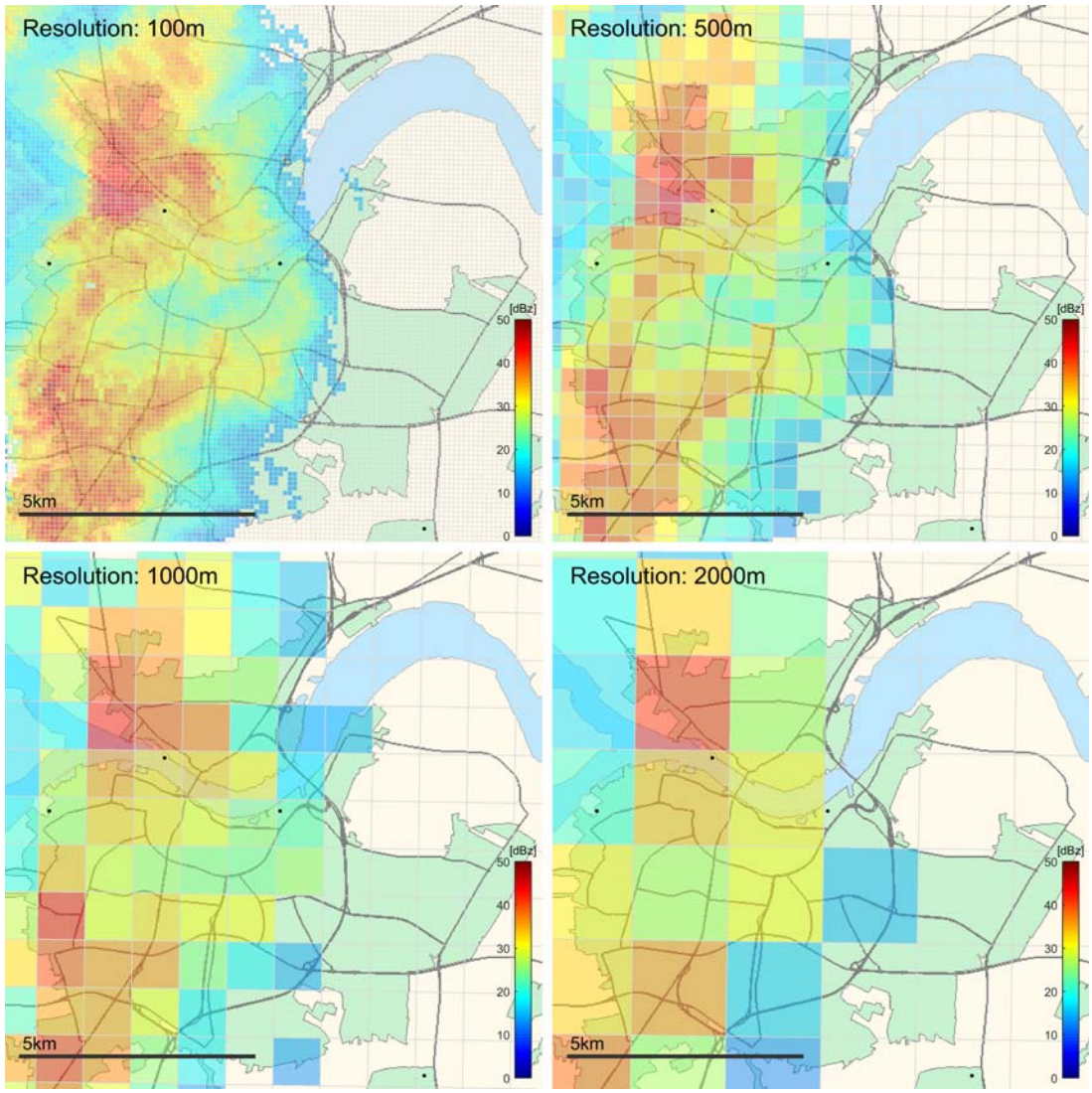

Figure 2.11 Example of radar reflectivity maps at four different Cartesian spatial resolutions over Aalborg, Denmark (Lat: 57.05, Lon: 9.92). The radar data were acquired with a Furuno WR-2100 dual-polarimetric X-band radar (Nielsen *et al.*, 2014) at 1 minute temporal resolution at 16:20:00 UTC on July 25, 2016. Black circles are rain gauges of the Danish Water Pollution Committee network. *Source*: Thorndahl *et al.* (2017).

2.4.3 Radar data quality, rainfall estimation, and radar data adjustment

The temporal resolution of radar data is determined by the recurrence time of the measurement by the radar at the same location. This ranges typically between 5 and 15 minutes for operational weather radars. Because radar measurement is an instantaneous measurement, information between the measurement times is

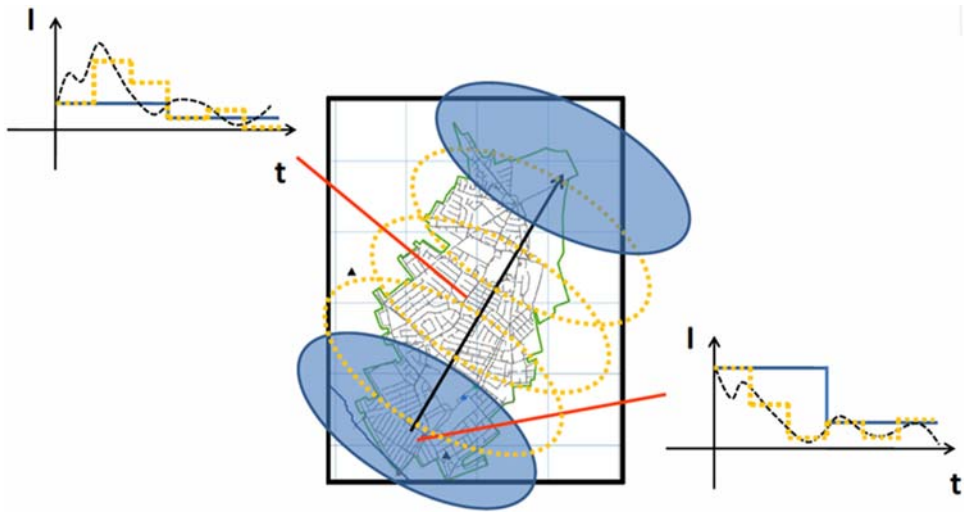

Figure 2.12 Enhancement of radar rainfall estimates for urban hydrology through optical flow temporal interpolation and Bayesian gauge-based adjustment. *Source*: Wang *et al.* (2015).

missing and can only be estimated – or is often considered as being constant between the time steps. This is frequently the case for data products from weather services.

In order to increase the temporal resolution of operational meteorological radar data, especially for urban hydrological applications, some authors have developed methods to interpolate between radar images (e.g. Fabry *et al.*, 1994; Jasper-Tönnies & Jessen, 2014; Thorndahl *et al.*, 2014; Wang *et al.*, 2015) (Figure 2.12). The governing principle in these interpolation methods is to apply the advection field of the rain, similar to a nowcasting procedure, and by resampling in space, to convert the spatial resolution into temporal resolution. The methods have been proven to give better local peak estimates of rainfall intensities as well as more accurate accumulated quantitative precipitation estimates in comparison with point ground observations. Jasper-Tönnies & Jessen (2014), Nielsen *et al.* (2014), Seo & Krajewski (2015) and Wang *et al.* (2015) have successfully converted data with a 5- or 10-minute resolution into a product with a 1-minute resolution for use in urban hydrological modelling (Figure 2.12).

Considering the advective nature of rain, it is also obvious that this advection correction yields a better estimate of the real precipitation. An accumulation of instantaneous radar data with e.g. a 5-minute sampling time interval may result in a 'fishbone' pattern (Figure 2.13).

The use of radar data requires that the data are of good quality. There are numerous items such as radar hardware calibration, clutter removal, overshooting/vertical profile correction, etc. (Li, 2020; Michelson *et al.*, 2005; Villarini & Krajewski, 2010), which have to be considered and may have to be corrected before radar reflectivity data can be converted into reliable rainfall intensities. A thorough quality check and potential correction are therefore required. Disturbances for a good radar measurement may be undesired reflections of mountains, high towers, air planes, ships, or wind turbines, attenuation by heavy rain or hail, snow or melting snow instead of rainfall, anomalous propagation conditions and others. Methods to test for these problems exist, and they are partly reduced by dual-polarization information from the new generation radars. The preprocessing of radar data by meteorological services usually only covers some of the above points.

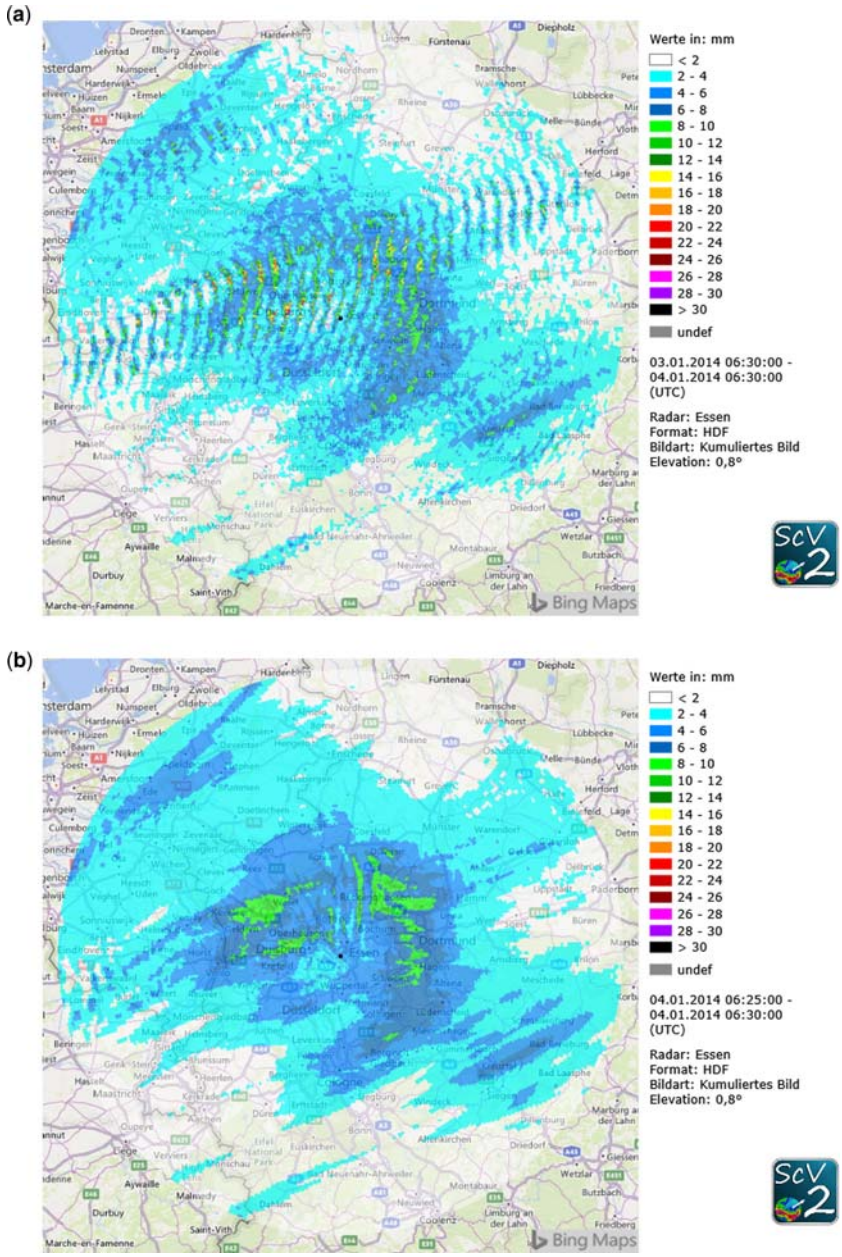

Figure 2.13 (a) Daily sum of rainfall depth (in mm) estimated from radar data measured from January 3, 2014 06:30 UTC to January 4, 2014 06:30 UTC in Essen, Germany with a 5-minute time step. Clearly visible is the 'fishbone' structure, due to the movement of the rainfall between the scanned images. (b) Image as above, but with a 1-minute temporal interpolation between each measured time step. *Source*: Thomas Einfalt (hydro & meteo GmbH).

Observed radar reflectivity can be converted into rain intensities, but comparison and adjustment with ground observations is required to produce valid quantitative precipitation estimates (QPE). This is most often referred to as radar rainfall adjustment or radar-rain gauge merging.

Rain gauges used for adjustment also need to be of high quality. Frequently observed shortcomings of rain gauge data are missing data, time shifts or differently set clocks, clogging of the gauge, data transmission drop outs, gauge calibration errors, local wind effects around gauges leading to measurement errors, or gauge sampling errors (e.g. Ciach, 2003; Gires *et al.*, 2014; Villarini *et al.*, 2008). To avoid random or systematic errors, such effects need to be eliminated before rain gauge data are used to adjust radar rainfall. Automatic procedures for these tasks exist (Einfalt & Frerk, 2011), but data controlled and corrected by experienced observers still give better results.

The relation between measured radar reflectivity, Z (in mm^6/m^3 or dBZ) and rain intensity, R (mm/h) as the target unit for hydrology depends on the drop size distribution (DSD) of the observed precipitation. As documented by numerous authors (e.g. Marshall & Palmer, 1948; Uijlenhoet, 2001), the most commonly used conversion for single polarization radars is to apply a two-parameter power-law relationship to describe the relation between rain intensity and radar reflectivity, named the *Z-R* relationship: $Z = aR^b$ (Figure 2.14). Since the power-law parameters vary with the DSD shape, i.e. the type of rain, they are not constant in time. One solution is to adjust the *Z-R* relationship continuously by use of ground observations. It is however more common to apply a fixed *Z-R* relationship and perform a posteriori bias adjustment.

Whereas traditional *Z-R* conversion is well documented in numerous applications of radar, there are recent advances in the application of dual-polarized radars which enable more accurate QPE assessment using polarimetric parameters (e.g. Anagnostou & Anagnostou, 2008; Anagnostou *et al.*, 2004; Bringi & Chandrasekar, 2001; Bringi *et al.*, 2011; Li, 2020; Mishra *et al.*, 2016; Ochoa-Rodriguez *et al.*, 2019; Scarchilli *et al.*, 1993; Simpson & Fox, 2018). Polarization of a radar signal characterizes the orientation of the electric field (both transmitted and received). Dual-polarimetric radars transmit a radar signal alternately in horizontal (H) and vertical (V) polarization. Depending on the shape of the rain drops, two different signals are received: reflectivities Z_{HH} and Z_{VV}. Additionally, the phase of the horizontally and vertically polarized return signals, f_{HH} and f_{VV}, are measured (Illingworth, 2004). Four parameters can be defined based on the polarimetric measurements: differential reflectivity Z_{dr}, linear depolarization ratio

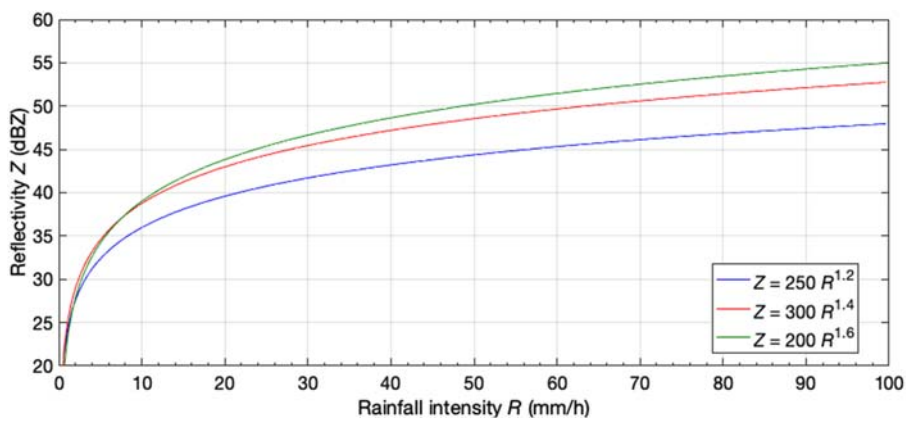

Figure 2.14 *Z-R* relationships of Marshall & Palmer (1948). *Source*: adapted from Marshall & Palmer (1948).

L_{dr}, co-polar correlation coefficient ρ_{hv} and the specific differential phase K_{dp} (Illingworth, 2004). K_{dp} is proportional to the product of rainwater content and the mass-weighted mean diameter (Bringi & Chandrasekar, 2001) and thus can be used to estimate rainfall intensities. The advantage of using K_{dp} for rainfall intensity estimation is that it is more sensitive to the raindrop shape, thus rainfall intensity can be estimated from K_{dp} in the case of rain/hail mixture. As soon as the hydrometeors are spherical or quasi-spherical, K_{dp} is about 0°/km (hail, light rain). Another advantage of using K_{dp} is that it is independent of radar calibration and not sensitive to attenuation, an issue of particular importance at X-band frequency. K_{dp} can only be estimated for medium to high rainfall rates (Otto & Russchenberg, 2011).

Many different methods for adjusting rain intensities estimated from radar reflectivities have been developed, and several profound review papers on different adjustment/merging techniques related to hydrological applications exist (e.g. Goudenhoofdt & Delobbe, 2009; McKee & Binns, 2016; Ochoa-Rodriguez *et al.*, 2019; Wang *et al.*, 2013). For specific details we refer to these. The most widely applied methods are presented hereafter.

A basic method of adjusting radar rainfall data to gauge data implies a temporally and spatially uniform relationship between both measurements. It has been proposed by Smith & Krajewski (1991) as the concept of mean field bias (MFB) adjustment. The concept is to estimate the ratio between accumulated rainfall depth in several ground observation points (rain gauges) and accumulated radar rainfall in the corresponding points (grid cells). Under the above-mentioned simplifying assumption, the whole radar field is multiplied by one MFB factor.

The processing of QPE for urban applications requires that the DSD is considered to be spatially heterogeneous and also not constant in time. For this, more sophisticated methods have been developed which either preprocess the station data by an interpolation process or perform an interpolation of the obtained relations between gauges and collocated radar pixels.

The optimal temporal integration period or spatial aggregation level is, to a large extent, dependent on the representativeness of the gauges (gauge network density) to capture the temporal and spatial variability of the rain (e.g. Gires *et al.*, 2014). It is difficult to recommend specific gauge network densities for radar rainfall adjustment since the optimal value will depend on storm type, homogeneity of the rain gauge network, orographic features of the rain, adjustment methods, etc. McKee & Binns (2016) suggest conducting a sensitivity analysis to identify the effect of gauge density on rainfall estimation.

Spatial variability adjustment approaches and geostatistical merging of radar and rain gauge data have been developed to account for range dependence issues as well as heterogeneous DSDs. They are widely applied for QPE. The concept here is to merge the spatial variability of the radar rainfall fields into the interpolated rain gauge precipitation fields to increase the spatial resolution of this product. The interpolation can be performed by many different spatial interpolation methods e.g. variations of kriging (Goudenhoofdt & Delobbe, 2009; Krajewski, 1987; Ochoa-Rodriguez *et al.*, 2019; Sinclair & Pegram, 2005), by inverse distance weighting or Thiessen polygon weighting (Haberlandt, 2007; Johnson *et al.*, 1999) or Bayesian methods (Ochoa-Rodriguez *et al.*, 2015, 2019; Todini, 2001; Wang *et al.*, 2015). The kriging-based methods rely on variograms for describing the spatial dependence in rainfall fields and are in general more computationally demanding than inverse distance weighting methods. The latter are therefore often used in real-time operation. A recent new development is the use of convective rain cells as singularity elements to be integrated in the rain gauge – radar interpolation method for a more accurate estimation of fine-scale extreme rainfall intensities, which are of importance for many urban water applications. Example results of the application of some rain gauge – radar adjustment, merging and interpolation approaches are shown in Figure 2.15.

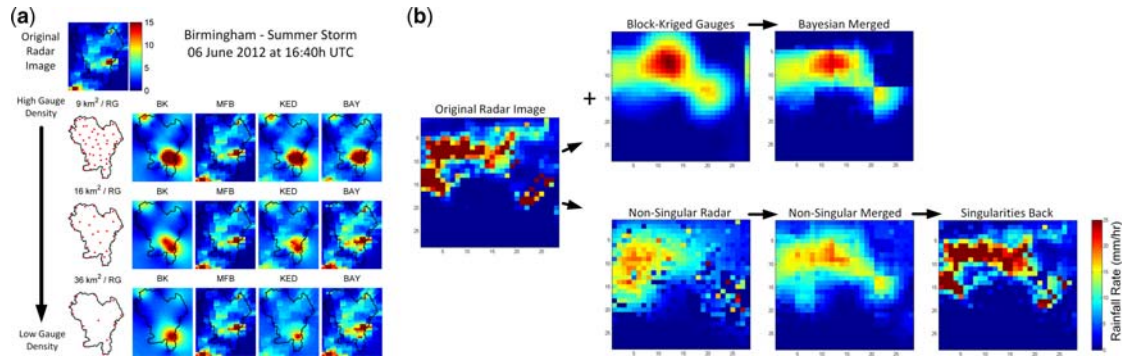

Figure 2.15 Example results of radar data adjustment approaches. (a) Original radar image is shown in the top row for an event measured in Birmingham on 06 June 2012, with rain gauge (RG) location and density on the left side, and the following four columns with (i) block-kriged (BK) interpolated rain gauge records, (ii) mean field bias (MFB), (iii) kriging with external drift (KED) and (iv) Bayesian combination (BAY). Radar records were available at 1-km^2/5-min resolution, while rain gauge records were available at 2-min temporal resolution. (b) Singularity-sensitive gauge-based radar rainfall adjustment methods by Wang *et al.* (2015). *Sources*: (a) adapted from Ochoa-Rodriguez (2017) and (b) adapted from Wang *et al.* (2015).

2.4.4 Summary

Weather radar nowadays is an established tool to provide rainfall information with a high temporal and spatial resolution. The shortcomings of radar, in particular the uncertain estimate of the absolute amount of precipitation, has to be taken care of by combining the radar information with rain gauge measurements in an appropriate manner. Radar rainfall estimates are – as an indirect measurement – prone to uncertainties associated with variability in drop size distribution, partial beam filling, overshooting, and signal attenuation. These effects need to be considered and corrected for where possible. A new way to reduce these uncertainties is by using polarimetric signals, another way is by reducing the distance to the radar, by increasing the density of the radar network. The quality of radar data adjustment in turn depends on the density and quality of the rain gauge network. The optimal temporal integration period or spatial aggregation level for radar adjustment is directly related to the ability of the rain gauge network to capture the temporal and spatial rainfall variability. For practice applications in urban hydrology, it is most often important to apply a powerful software package which is able to cover the above-mentioned work tasks for a high quality of radar measurement data.

2.5 MICROWAVE LINKS

Another emerging method for rainfall monitoring is the use of microwave links. A microwave link consists of two antennas, one sending and one receiving unit, typically a few hundred metres up to 15 km apart. Microwave links are used for mobile telephone communication, they operate around a frequency of 7–40 GHz and the link length is mostly limited to a maximum of 5–10 km. There is quite a dense network available in some countries. However, in others, this might be limited. As an estimate of the density of the microwave link network, a density of at least 0.3 links/km^2 can be assumed for European countries, according to Chwala *et al.* (2012). For example, in the Netherlands (35,500 km^2) the total number of link paths is at least 8000 and for many of those link paths, the microwave links measure in both directions (Overeem *et al.*, 2011).

The information sent over these links also has to travel through rain, which causes attenuation of the signal. The magnitude of the received power is mostly stored by the network operators and can thus be used to calculate the total integrated attenuation over the link path, from which the path averaged rainfall intensity can be estimated.

Research in this field started with research set-ups (e.g. Grum *et al.*, 2005; Holt *et al.*, 2003; Krämer *et al.*, 2005; Leijnse *et al.*, 2007a; Rahimi *et al.*, 2003, 2004, 2006; Ruf *et al.*, 1996; Upton *et al.*, 2005), but in recent years, data from commercial cellular networks have been used to estimate rainfall intensities (e.g. Chwala *et al.*, 2012; Leijnse *et al.*, 2007b; Messer *et al.*, 2006; Overeem *et al.*, 2011; Zinevich *et al.*, 2008). A limitation is the availability of the data, which could range from (near) real-time up to only on a daily or even weekly basis. Moreover, it can be hard to gain access to commercial microwave link data.

The microwave links can be used as a standalone estimator of the rainfall (e.g. Leijnse *et al.*, 2007b; Zinevich *et al.*, 2008), or can be combined with rain gauges and even radar measurements (e.g. Cummings *et al.*, 2009) to give better rainfall estimations at ground level. The links can also be used as an attenuation indicator for attenuation correction of the radar measurements. The network of these links is mostly more dense over urban areas than elsewhere, which could thus be an advantage for the correction of the radar estimates for urban hydrological applications since there are mostly only a limited number of rain gauges available in the city centre. Other advantages of microwave links are that they are mostly clutter free and very close to the ground compared to radar scans. Finally, the power law equation used to compute rainfall intensity from attenuation is almost linear, whereas the *ZR* relation employed in radar meteorology is nonlinear.

2.6 SUMMARY AND TRANSITION

This chapter introduced the most common rain measuring devices: a few for local measurements (rain gauges and disdrometers) and the weather radar for larger measurements over urban catchments. Both present advantages and disadvantages and can always be combined together to reduce their weaknesses (Figure 2.16).

A municipality or utility can easily purchase, install, calibrate, and operate a network of weighing or tipping bucket rain gauges with specifically trained employees. Access to radar data, either in real time

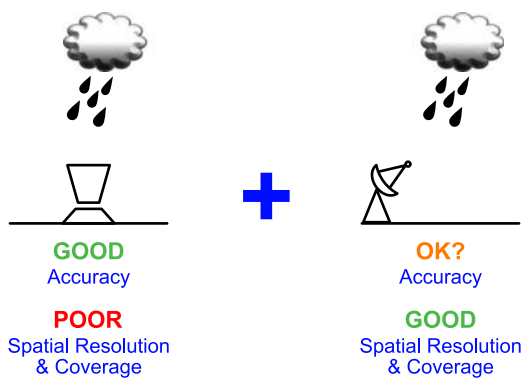

Figure 2.16 Advantages and disadvantages of local rainfall measurements (rain gauges and disdrometers) and weather radar data, where rainfall adjustment, interpolation or merging methods aim to combine the advantages. *Source*: Patrick Willems (KU Leuven).

or off-line, can be obtained by contracting with: (i) either national or regional meteorological services, or (ii) a service provider company. It is less common practice for a municipality or utility to own and operate their own radar. However, possible future dissemination of small X-band radars may change the practice in the future, likely in association with a service provider to calibrate and validate radar data.

Once rain has been measured, runoff processes will start. The following chapter is therefore devoted to discharge measurements within sewer pipes to accurately quantify flows inside the network itself.

REFERENCES

Abd Elbasit M. A. M., Yasuda H. & Salmi A. (2011). Application of piezoelectric transducers in simulated rainfall erosivity assessment. *Hydrological Sciences Journal*, **56**(1), 187–194. doi: 10.1080/02626667.2010.546359.

Adami A. & Da Deppo L. (1985). On the systematic errors of tipping bucket recording rain gauges. *Proceedings of the International Workshop on the Correction of Precipitation Measurements*, 1–3 April 1985, Zürich, Switzerland.

Alter C. J. (1937). Shielded storage precipitation gauges. *Monthly Weather Review*, **65**(7), 262–265. doi: 10.1175/1520-0493(1937)65<262:SSPG>2.0.CO;2.

Anagnostou M. N. & Anagnostou E. N. (2008). Chapter 12: Performance of algorithms for rainfall retrieval from dual-polarization X-band radar measurements. In *Precipitation: Advances in Measurement, Estimation and Prediction*, S. C. Michaelis (ed.), Springer Verlag, Berlin Heidelberg (Germany), pp. 313–342. ISBN 978-3-540-77654-3.

Anagnostou E. N., Anagnostou M. N., Krajewski W. F., Kruger A. & Miriovsky B. J. (2004). High-resolution rainfall estimation from X-band polarimetric radar measurements. *Journal of Hydrometeorology*, **5**(1), 110–128. doi: 10.1175/1525-7541(2004)005<0110:HREFXP>2.0.CO;2.

Battaglia A., Rustemeier E., Tokay A., Blahak U. & Simmer C. (2010). PARSIVEL snow observations: a critical assessment. *Journal of Atmospheric and Oceanic Technology*, **27**(2), 333–344. doi: org/10.1175/2009JTECHA1332.1.

Belenguer F. M., Martínez-Millana A., Salcedo A. M., Sánchez V. M. & Anaya M. J. P. (2020). Disdrometer performance optimization for use in urban settings based on the parameters that affect the measurements. *Symmetry*, **12**(2), 303, 19 p. doi: 10.3390/sym12020303.

Bertrand-Krajewski J.-L., Laplace D., Joannis C. & Chebbo G. (2000). *Mesures en hydrologie urbaine et assainissement [Measurements in urban hydrology and sewer systems]*. Editions Technique et Documentation, Paris (France), 794 p. ISBN 978-2-7430-0380-4. (in French).

Braak C. (1945). *Invloed van den wind op regenwaarnemingen [Wind influence on rain gauge measurements]*. 's-Gravenhage (The Netherlands): Royal Dutch Meteorological Institute of the Netherlands, Mededelingen en Verhandelingen, Rijksuitgeverij, volume 48, report 102. (in Dutch).

Brawn D. & Upton G. (2008). Estimation of an atmospheric gamma drop size distribution using disdrometer data. *Atmospheric Research*, **87**(1), 66–79. doi: 10.1016/j.atmosres.2007.07.006.

Bringi V. N. & Chandrasekar V. (2001). *Polarimetric Doppler Weather Radar*. Cambridge University Press, Cambridge (UK), 664 p. ISBN 978-0521019552.

Bringi V. N., Rico-Ramirez M. A. & Thurai M. (2011). Rainfall estimation with an operational polarimetric C-band radar in the United Kingdom: comparison with a gauge network and error analysis. *Journal of Hydrometeorology*, **12**(5), 935–954. doi: 10.1175/JHM-D-10-05013.1.

Chwala C., Gmeiner A., Qiu W., Hipp S., Nienaber D., Siart U., Eibert T., Pohl M., Seltmann J., Fritz J. & Kunstmann H. (2012). Precipitation observation using microwave backhaul links in the alpine and pre-alpine region of southern Germany. *Hydrology and Earth System Sciences Discussions*, **9**(1), 741–776. doi: 10.5194/hessd-9-741-2012.

Ciach G. J. (2003). Local random errors in tipping-bucket rain gauge measurements. *Journal of Atmospheric and Oceanic Technology*, **20**(5), 752–759. doi: 10.1175/1520-0426(2003)20<752:LREITB>2.0.CO;2.

Cummings R. J., Upton G. J. G., Holt A. R. & Kitchen M. (2009). Using microwave links to adjust the radar rainfall field. *Advances in Water Resources*, **32**(7), 1003–1010. doi: 10.1016/j.advwatres.2008.08.010.

Desaulnier-Soucy N., Lovejoy S. & Schertzer D. (2001). The HYDROP experiment: an empirical method for the determination of the continuum limit in rain. *Atmospheric Research*, **59–60**, 163–197. doi: 10.1016/S0169-8095(01)00115-6.

Duchon C. E. & Essenberg G. R. (2001). Comparative rainfall observations from pit and aboveground rain gauges with and without wind shields. *Water Resources Research*, **37**(12), 3253–3263. doi: 10.1029/2001WR000541.

DWD (2018). *Radar Products*. Deutscher Wetterdienst, Offenbach (Germany). Available at https://www.dwd.de/EN/ourservices/radar_products/radar_products.html (accessed 06 October 2020).

Einfalt T. & Frerk I. (2011). On the influence of high quality rain gauge data for radar-based rainfall estimation. *Proceedings of the 12th ICUD – International Conference on Urban Drainage*, 11–15 September, Porto Alegre, Brazil.

Ellis R. A., Sandford A. P., Jones G. E., Richards J., Petzing J. & Coupland J. M. (2006). New laser technology to determine present weather parameters. *Measurement Science and Technology*, **17**, 1715–1722. doi: 10.1088/0957-0233/17/7/009.

Fabry F., Bellon A., Duncan M. R. & Austin G. L. (1994). High resolution rainfall measurements by radar for very small basins: the sampling problem re-examined. *Journal of Hydrology*, **161**(1–4), 415–428. doi: 10.1016/0022-1694(94)90138-4.

Frasson R. P. D. M., da Cunha L. K. & Krajewski W. F. (2011). Assessment of the Thies optical disdrometer performance. *Atmospheric Research*, **101**(1–2), 237–255. doi: 10.1016/j.atmosres.2011.02.014.

Gires A., Tchiguirinskaia I., Schertzer D., Schellart A., Berne A. & Lovejoy S. (2014). Influence of small scale rainfall variability on standard comparison tools between radar and rain gauge data. *Atmospheric Research*, **138**, 125–138. doi: 10.1016/j.atmosres.2013.11.008.

Goudenhoofdt E. & Delobbe L. (2009). Evaluation of radar-gauge merging methods for quantitative precipitation estimates. *Hydrology and Earth System Sciences Discussions*, **13**(2), 195–203. doi: 10.5194/hess-13-195-2009.

Grum M., Krämer S., Verworn H.-R. & Redder A. (2005). Combined use of point rain gauges, radar, microwave link and level measurements in urban hydrological modelling. *Atmospheric Research*, **77**(1–4), 313–321. doi: 10.1016/j.atmosres.2004.10.013.

Haberlandt U. (2007). Geostatistical interpolation of hourly precipitation from rain gauges and radar for a large-scale extreme rainfall event. *Journal of Hydrology*, **332**(1–2), 144–157. doi: 10.1016/j.jhydrol.2006.06.028.

Habib E., Meselhe E. A. & Aduvala A. V. (2008). Effect of local errors of tipping-bucket rain gauges on rainfall-runoff simulations. *Journal of Hydrologic Engineering*, **13**(6), 488–496. doi: 10.1061/(ASCE)1084-0699(2008)13:6(488).

Holt A. R., Kuznetsov G. G. & Rahimi A. R. (2003). Comparison of the use of dual-frequency and single frequency attenuation for the measurement of rainfall along a microwave link. *IEE Proceedings of the Microwaves Antennas and Propagation*, **150**(5), 315–320. doi: 10.1049/ip-map:20030616.

Humphrey M. D., Istok J. D., Lee J. Y., Hevesi J. A. & Flint A. L. (1997). A new method for automated dynamic calibration of tipping-bucket rain gauges. *Journal of Atmospheric and Oceanic Technology*, **14**(6), 1513–1519. doi: 10.1175/1520-0426(1997)014<1513:ANMFAD>2.0.CO;2.

Illingworth A. (2004). Improved precipitation rates and data quality by using polarimetric measurements. In *Weather Radar – Principles and Advanced Applications*, P. Meischner (ed.), Springer, Berlin, Heidelberg (Germany), pp. 130–166. ISBN 978-3540003281.

ISO (2019). *ISO 19926-1:2019 Meteorology — Weather Radar — Part 1: System Performance and Operation*. World Meteorological Organisation, Geneva (Switzerland), 93 p.

Jaffrain J. & Berne A. (2011). Experimental quantification of the sampling uncertainty associated with measurements from PARSIVEL disdrometers. *Journal of Hydrometeorology*, **12**(3), 352–370. doi: 10.1175/2010JHM1244.1.

Jaffrain J. & Berne A. (2012a). Influence of the subgrid variability of the raindrop size distribution on radar rainfall estimators. *Journal of Applied Meteorology and Climatology*, **51**(4), 780–785. doi: 10.1175/JAMC-D-11-0185.1.

Jaffrain J. & Berne A. (2012b). Quantification of the small-scale spatial structure of the raindrop size distribution from a network of disdrometers. *Journal of Applied Meteorology and Climatology*, **51**(5), 941–953. doi: 10.1175/JAMC-D-11-0136.1.

Jasper-Tönnies A. & Jessen M. (2014). Improved radar QPE with temporal interpolation using an advection scheme. *Proceedings of ERAD 2014 – The 8th European Conference on Radar in Meteorology and Hydrology*, 1–5 September, Garmisch-Partenkirchen, Germany, 6 p.

Johnson D., Smith M., Koren V. & Finnerty B. (1999). Comparing mean areal precipitation estimates from NEXRAD and rain gauge networks. *Journal of Hydrologic Engineering*, **4**(2), 117–124. doi: 10.1061/(ASCE)1084-0699(1999)4:2(117).

Joss J. & Waldvogel A. (1967). Ein Spektrograph für Niederschlagstropfen mit automatischer Auswertung [A spectrograph for raindrops with automatic interpretation]. *Pure and Applied Geophysics*, **68**, 240–246. doi: 10.1007/BF00874898. (in German).

Krajewski W. F. (1987). Cokriging radar-rainfall and rain gage data. *Journal of Geophysical Research Atmospheres*, **92**(8), 9571–9580. doi: 10.1029/JD092iD08p09571.

Krajewski W. F., Kruger A., Caracciolo C., Golé P., Barthes L., Creutin J.-D., Delahaye J.-Y., Nikolopoulos E. I., Ogden F. & Vinson J.-P. (2006). DEVEX-disdrometer evaluation experiment: basic results and implications for hydrologic studies. *Advances in Water Resources*, **29**(2), 311–325. doi: 10.1016/j.advwatres.2005.03.018.

Krämer S., Verworn H.-R. & Redder A. (2005). Improvement of X-band radar rainfall estimates using a microwave link. *Atmospheric Research*, **77**(1–4), 278–299. doi: 10.1016/j.atmosres.2004.10.028.

Kruger A. & Krajewski W. F. (2002). Two-dimensional video disdrometer: a description. *Journal of Atmospheric and Oceanic Technology*, **19**(5), 602–617. doi: 10.1175/1520-0426(2002)019<0602:TDVDAD>2.0.CO;2.

Kvicera V. & Grabner M. (2006). Dynamic calibration of tipping-bucket rain gauges and rainfall intensity data processing. *Proceedings of EuCAP 2006 – 1st European Conference on Antennas and Propagation*, 6–10 November, Nice, France, pp. 1–5. doi: 10.1109/EUCAP.2006.4584771.

La Barbera P., Lanza L. G. & Stagi L. (2002). Tipping bucket mechanical errors and their influence on rainfall statistics and extremes. *Water Science and Technology*, **45**(2), 1–9. doi: 10.2166/wst.2002.0020.

Larkin H. (1947). A comparison of the Alter and Nipher shields for precipitation gauge. *Bulletin of the American Meteorological Society*, **28**(4), 200–201.

Leijnse H., Uijlenhoet R. & Stricker J. N. M. (2007a). Hydrometeorological application of a microwave link: 2. Precipitation. *Water Resources Research*, **43**(4), W04417, 9 p. doi: 10.1029/2006WR004989.

Leijnse H., Uijlenhoet R. & Stricker J. N. M. (2007b). Rainfall measurement using radio links from cellular communication networks. *Water Resources Research*, **43**(3), W03201, 6 p. doi: 10.1029/2006WR005631.

Leijnse H., Uijlenhoet R., van de Beek C. Z., Overeem A., Otto T., Unal C. M. H., Dufournet Y., Russchenberg H. W. J., Figueras i Ventura J., Klein Baltink H. & Holleman I. (2010). Precipitation measurement at CESAR, The Netherlands. *Journal of Hydrometeorology*, **11**(6), 1322–1329. doi: 10.1175/2010JHM1245.1.

Lengfeld K., Clemens M., Münster H. & Ament F. (2014). Performance of high-resolution X-band weather radar networks – the PATTERN example. *Atmospheric Measurement Techniques*, **7**(12), 4151–4166, doi: 10.5194/amt-7-4151-2014.

Li X. (2020). *Radar-Based Fine-Scale Rainfall Estimation and Probabilistic Nowcasting of Urban Flooding*. PhD dissertation, KU Leuven, Leuven, Belgium.

Löffler-Mang M. & Joss J. (2000). An optical disdrometer for measuring size and velocity of hydrometeors. *Journal of Atmospheric and Oceanic Technology*, **17**(2), 130–139. doi: 10.1175/1520-0426(2000)017<0130:AODFMS>2.0.CO;2.

Luyckx G. & Berlamont J. (2001). Simplified method to correct rainfall measurements from tipping bucket rain gauges. *Proceedings of the Specialty Symposium on Urban Drainage Modeling at the World Water and Environmental Resources Congress*, 20–24 May, Orlando, FL, USA, pp. 767–776. doi: 10.1061/40583(275)72.

Marsalek J. (1981). Calibration of the tipping bucket raingauge. *Journal of Hydrology*, **53**(3–4), 343–354. doi: 10.1016/0022-1694(81)90010-X.

Marshall J. S. & Palmer W. M. (1948). The distribution of raindrops with size. *Journal of Meteorology*, **5**(4), 165–166. doi: 10.1175/1520-0469(1948)005<0165:TDORWS>2.0.CO;2.

McKee J. L. & Binns A. D. (2016). A review of gauge–radar merging methods for quantitative precipitation estimation in hydrology. *Canadian Water Resources Journal*, **41**(1–2), 186–203. doi: 10.1080/07011784.2015.1064786.

Messer H. A., Zinevich A. & Alpert P. (2006). Environmental monitoring by wireless communication networks. *Science*, **312**(5774), 713. doi: 10.1126/science.1120034.

Michelson D., Einfalt T., Holleman I., Gjertsen U., Friedrich K., Haase G., Lindskog M. & Jurczyk A. (2005). *Weather Radar Data Quality in Europe: Quality Control and Characterisation*. Review, COST Action 717 - Use of radar observations in hydrological and NWP models, Luxembourg.

Miriovsky B. J., Bradley A. A., Eichinger W. E., Krajewski W. F., Kruger A., Nelson B. R., Creutin J.-D., Lapetite J.-M., Lee G. W., Zawadzki I. & Ogden F. L. (2004). An experimental study of small-scale variability of radar reflectivity using disdrometer observations. *Journal of Applied Meteorology and Climatology*, **43**(1), 106–118. doi: 10.1175/1520-0450(2004)043<0106:AESOSV>2.0.CO;2.

Mishra K. V., Krajewski W. F., Goska R., Ceynar D., Seo B.-C., Kruger A., Niemeier J. J., Galvez M. B., Thurai M., Bringi V. N., Tolstoy L., Kucera P. A., Petersen W. A., Grazioli J. & Pazmany A. L. (2016). Deployment and performance analyses of high-resolution Iowa XPOL radar system during the NASA IFloodS campaign. *Journal of Hydrometeorology*, **17**(2), 455–479. doi: 10.1175/JHM-D-15-0029.1.

Neff E. L. (1977). How much rain does a rain gage gauge? *Journal of Hydrology*, **35**(3–4), 213–220. doi: 10.1016/0022-1694(77)90001-4.

Nielsen J. E., Thorndahl S. & Rasmussen M. R. (2014). A numerical method to generate high temporal resolution precipitation time series by combining weather radar measurements with a nowcast model. *Atmospheric Research*, **138**, 1–12. doi: 10.1016/j.atmosres.2013.10.015.

Niemczynowicz J. (1986). The dynamic calibration of tipping-bucket raingauges. *Nordic Hydrology*, **17**(3), 203–214. doi: 10.2166/nh.1986.0013.

Ochoa-Rodriguez S. (2017). *Rainfall Estimates for Urban Drainage Modelling: An Investigation into Resolution Requirements and Radar-Rain Gauge Data Merging at the Required Resolutions*. PhD Thesis, Imperial College London, London, UK.

Ochoa-Rodriguez S., Wang L.-P., Gires A., Pina L. R., Reinoso Rondinel R., Bruni G., Ichiba A., Gaitan S., Cristiano E., van Assel J., Kroll S., Murla-Tuyls D., Tisserand B., Schertzer D., Tchiguirinskaia I., Onof C., Willems P. & ten Veldhuis J. A. E. M.-C. (2015). Impact of spatial and temporal resolution of rainfall inputs on urban hydrodynamic modelling: a multi-catchment investigation. *Journal of Hydrology*, **531**(2), 389–407. doi: 10.1016/j.jhydrol.2015.05.035.

Ochoa-Rodriguez S., Wang L.-P., Willems P. & Onof C. (2019). A review of radar-rain gauge data merging methods and their potential for urban hydrological applications. *Water Resources Research*, **55**(8), 6356–6391. doi: 10.1029/2018WR023332.

Otto T. & Russchenberg H. W. J. (2011). Estimation of specific differential phase and differential backscatter phase from polarimetric weather radar measurements of rain. *IEEE Geoscience and Remote Sensing Letters*, **8**(5), 988–992, doi:10.1109/LGRS.2011.2145354.

Overeem A., Leijnse H. & Uijlenhoet R. (2011). Measuring urban rainfall using microwave links from commercial cellular communication networks. *Water Resources Research*, **47**(12), W12505, 16 p. doi: 10.1029/2010WR010350.

Pedersen L., Jensen N. E. & Madsen H. (2010). Calibration of local area weather radar - Identifying significant factors affecting the calibration. *Atmospheric Research*, **97**(1–2), 129–143. doi: 10.1016/j.atmosres.2010.03.016.

Rahimi A. R., Holt A. R., Upton G. J. G. & Cummings R. J. (2003). The use of dual-frequency microwave links for measuring path-averaged rainfall. *Journal of Geophysical Research Atmospheres*, **108**(15), 4467, 12 p. doi: 10.1029/2002JD003202.

Rahimi A. R., Upton G. J. G. & Holt A. R. (2004). Dual-frequency links - a complement to gauges and radar for the measurement of rain. *Journal of Hydrology*, **288**(1–2), 3–12. doi: 10.1016/j.jhydrol.2003.11.008.

Rahimi A. R., Holt A. R., Upton G. J. G., Krämer S., Redder A. & Verworn H.-R. (2006). Attenuation calibration of an X-band weather radar using a microwave link. *Journal of Atmospheric and Oceanic Technology*, **23**(3), 395–405. doi: 10.1175/JTECH1855.1.

Rico-Ramirez M. A., Liguori S. & Schellart A. N. A. (2015). Quantifying radar-rainfall uncertainties in urban drainage flow modelling. *Journal of Hydrology*, **528**, 17–28. doi: 10.1016/j.jhydrol.2015.05.057.

Ruf C. S., Aydin K., Mathur S. & Bobak J. P. (1996). 35-GHz dual-polarization propagation link for rain-rate estimation. *Journal of Atmospheric and Oceanic Technology*, **13**(2), 419–425. doi: 10.1175/1520-0426(1996)013<0419:GDPPLF>2.0.CO;2.

Scarchilli G., Goroucci E., Chandrasekar V. & Seliga T. A. (1993). Rainfall estimation using polarimetric techniques at C-band frequencies. *Journal of Applied Meteorology and Climatology*, **32**(6), 1150–1160. doi: 10.1175/1520-0450(1993)032<1150:REUPTA>2.0.CO;2.

Seo B.-C. & Krajewski W. F. (2015). Correcting temporal sampling error in radar-rainfall: effect of advection parameters and rain storm characteristics on the correction accuracy. *Journal of Hydrology*, **531**(2), 272–283. doi: 10.1016/j.jhydrol.2015.04.018.

Sevruk B. (1996). Adjustment of tipping-bucket precipitation gauge measurements. *Atmospheric Research*, **42**(1–4), 237–246. doi: 10.1016/0169-8095(95)00066-6.

Simpson M. J. & Fox N. I. (2018). Dual-polarized quantitative precipitation estimation as a function of range. *Hydrology and Earth System Sciences*, **22**(6), 3375–3389. doi: 10.5194/hess-22-3375-2018.

Sinclair S. & Pegram G. (2005). Combining radar and rain gauge rainfall estimates using conditional merging. *Atmospheric Science Letters*, **6**(1), 19–22. doi: 10.1002/asl.85.

Smith J. A. & Krajewski W. F. (1991). Estimation of the mean field bias of radar rainfall estimates. *Journal of Applied Meteorology and Climatology*, **30**(4), 397–412. doi: 10.1175/1520-0450(1991)030<0397:EOTMFB>2.0.CO;2.

Strangeways I. C. (2007). *Precipitation – Theory, Measurement and Distribution*. Cambridge University Press, Cambridge (UK), 302 p. ISBN 978-0521851176.

Tapiador F. J., Checa R. & de Castro M. (2010). An experiment to measure the spatial variability of rain drop size distribution using sixteen laser disdrometers. *Geophysical Research Letters*, **37**(16), L16803, 6 p. doi: 10.1029/2010GL044120.

Thorndahl S. & Rasmussen M. R. (2012). Marine X-band weather radar data calibration. *Atmospheric Research*, **103**, 33–44. doi: 10.1016/j.atmosres.2011.04.023.

Thorndahl S., Nielsen J. E. & Rasmussen M. R. (2014). Bias adjustment and advection interpolation of long-term high resolution radar rainfall series. *Journal of Hydrology*, **508**, 214–226. doi: 10.1016/j.jhydrol.2013.10.056.

Thorndahl S., Einfalt T., Willems P., Nielsen J. E., ten Veldhuis M.-C., Arnbjerg-Nielsen K., Rasmussen M. R. & Molnar P. (2017). Weather radar rainfall data in urban hydrology. *Hydrology and Earth System Sciences Discussions*, **21**(3), 1359–1380. doi: 10.5194/hess-21-1359-2017.

Thurai M., Petersen W. A., Tokay A., Schultz C. & Gatlin P. (2011). Drop size distribution comparisons between Parsivel and 2-D video disdrometers. *Advances in Geosciences*, **30**, 3–9. doi: 10.5194/adgeo-30-3-2011.

Todini E. (2001). A Bayesian technique for conditioning radar precipitation estimates to rain-gauge measurements. *Hydrology and Earth System Sciences*, **5**, 187–199. doi: 10.5194/hess-5-187-2001.

Tokay A., Kruger A. & Krajewski W. F. (2001). Comparison of drop size distribution measurements by impact and optical disdrometers. *Journal of Applied Meteorology and Climatology*, **40**(11), 2083–2097. doi: 10.1175/1520-0450(2001)040<2083:CODSDM>2.0.CO;2.

Uijlenhoet R. (2001). Raindrop size distributions and radar reflectivity–rain rate relationships for radar hydrology. *Hydrology and Earth System Sciences*, **5**(4), 615–628. doi: 10.5194/hess-5-615-2001.

Upton G. J. G., Holt A. R., Cummings R. J., Rahimi A. R. & Goddard J. W. F. (2005). Microwave links: The future for urban rainfall measurement? *Atmospheric Research*, **77**(1–4), 300–312. doi: 10.1016/j.atmosres.2004.10.009.

van de Beek C. Z., Leijnse H., Stricker J. N. M., Uijlenhoet R. & Russchenberg H. W. J. (2010). Performance of high-resolution X-band radar for rainfall measurement in The Netherlands. *Hydrology and Earth System Sciences Discussions*, **14**(2), 205–221. doi:10.5194/hess-14-205-2010.

Villarini G. & Krajewski W. F. (2010). Review of the different sources of uncertainty in single polarization radar-based estimates of rainfall. *Surveys in Geophysics*, **31**(1), 107–129. doi: 10.1007/s10712-009-9079-x.

Villarini G., Mandapaka P. V., Krajewski W. F. & Moore R. J. (2008). Rainfall and sampling uncertainties: A rain gauge perspective. *Journal of Geophysical Research Atmospheres*, **113**(11), D11102, 12 p. doi: 10.1029/2007JD009214.

Wagner A. (2009). *Literature Study on the Correction of Precipitation Measurements*. Bavarian State Institute of Forestry, Freising (Germany), Deliverable C1-Met-29 of the Life+ FutMon project, 32 p.

Wang L.-P., Ochoa-Rodríguez S., Simões N. E., Onof C. & Maksimović C. (2013). Radar-raingauge data combination techniques: a revision and analysis of their suitability for urban hydrology. *Water Science and Technology*, **68**(4), 737–747. doi: 10.2166/wst.2013.300.

Wang L.-P., Ochoa-Rodriguez S., van Assel J., Pina R. D., Pessemier M., Kroll S., Willems P. & Onof C. (2015). Enhancement of radar rainfall estimates for urban hydrology through optical flow temporal interpolation and Bayesian gauge-based adjustment. *Journal of Hydrology*, **531**(2), 408–426. doi: 10.1016/j.jhydrol.2015.05.049.

Wauben W. (2006). *KNMI contribution to the WMO laboratory intercomparison of rainfall intensity gauges*. De Bilt (The Netherlands): KNMI, Technical report TR-287, 174 p. Available at http://bibliotheek.knmi.nl/knmipubTR/TR287.pdf (accessed 06 Oct. 2020).

Willems P. (2001). Stochastic description of the rainfall input errors in lumped hydrological models. *Stochastic Environmental Research and Risk Assessment*, **15**, 132–152. doi: 10.1007/s004770000063.

WMO (2018a). *Guide to Instruments and Methods of Observation – Volume I: Measurement of Meteorological Variables*. World Meteorological Organization, Geneva (Switzerland), 573 p. ISBN 978-92-63-10008-5. Available at https://library.wmo.int/doc_num.php?explnum_id=10179 (accessed 18 June 2020).

WMO (2018b). *Guide to Instruments and Methods of Observation – Volume III: Observing Systems*. World Meteorological Organization, Geneva (Switzerland), 573 p. ISBN 978-92-63-10008-5. Available at https://library.wmo.int/doc_num.php?explnum_id=9872 (accessed 04 Oct. 2020).

Yang D., Goodison B. E., Metcalfe J. R., Louie P., Leavesley G. H., Emerson D. G., Hanson C. L., Golubev V. S., Elomaa E., Gunther T., Pangburn T., Kang E. & Milkovic J. (1999). Quantification of precipitation measurement discontinuity induced by wind shields on national gauge. *Water Resources Research*, **35**(2), 491–508. doi: 10.1029/1998WR900042.

Zinevich A., Alpert P. & Messer H. (2008). Estimation of rainfall fields using commercial microwave communication networks of variable density. *Advances in Water Resources*, **31**(11), 1470–1480. doi: 10.1016/j.advwatres.2008.03.003.